arXiv:2204.03277v1 [eess.IV] 7 Apr 2022

Recursive Frequency Selective Reconstruction of Non-Regularly Sampled Video Data

Markus Jonscher, Karina Jaskolka, Jürgen Seiler, and André Kaup
Multimedia Communications and Signal Processing
Friedrich-Alexander University Erlangen-Nürnberg (FAU), Cauerstr. 7, 91058 Erlangen, Germany

***Abstract*—High resolution images can be acquired using a non-regular sampling sensor which consists of an underlying low resolution sensor that is covered with a non-regular sampling mask. The reconstructed high resolution image is then obtained during post-processing. Recently, it has been shown that the temporal correlation between neighboring frames can be exploited in order to enhance the reconstruction quality of non-regularly sampled video data. In this paper, a new recursive multi-frame reconstruction approach is proposed in order to further increase the reconstruction quality. By using a new reference order, previously reconstructed frames can be used for the subsequent motion estimation and a new weighting function allows for the incorporation of multiple pixels projected onto the same position. With the new recursive multi-frame approach, a visually noticeable average gain in PSNR of up to 1.13 dB with respect to a state-of-the-art single-frame reconstruction approach can be achieved. Compared to the existing multi-frame approach, a gain of 0.31 dB is possible. SSIM results show the same behavior as PSNR results. Additionally, the pre-reconstruction step of the existing multi-frame approach can be avoided and the new algorithm is, in general, capable of real-time processing.**

I. Introduction

The fundamental work of Kotelnikov, Nyquist, Shannon, and Whittaker on sampling continuous band-limited signals [1] shows that these signals can be exactly restored from a set of regularly spaced samples if they are acquired with twice the highest frequency present in the regarded signal. However, in many important applications like imaging, medical imaging, or remote surveillance, the resulting rate is so high that far too many samples have to be acquired. Despite the advances in computational power, it may be either too costly or even physically impossible to build devices capable of acquiring such signals at the necessary rate. A few years ago, Compressed Sensing [2], [3] has been introduced as a new framework for signal acquisition and sensor design. It achieves a large reduction in sampling and computational costs for sensing signals that have a sparse representation in another domain. The idea behind Compressed Sensing is to directly acquire the data in a compressed form which means a lower sampling rate rather than first sample it at a high rate and compress afterwards. Compressed Sensing is used for instance in single-pixel cameras [4], where a scene is acquired by random projections instead of collecting the pixels. The reconstructed high resolution image can be obtained afterwards.

Another possibility to obtain a high resolution image and to reduce the costs and storage space of the data acquisition at the same time has been shown in [5], where a low resolution sensor is covered with a non-regular sampling mask. The basic idea of this approach is shown in Figure 1. On the left, a high resolution sensor that gives the high resolution image $f[m,n]$ is displayed. The area of the sensor that is sensitive to light is denoted in light-gray and (m,n) depict the spatial coordinates on this high resolution grid. In many applications like multi-view scenarios or mobile devices it is of interest to reduce hardware costs or the energy consumption. Therefore, a low resolution sensor with fewer read-out circuits may be employed which is shown in the middle. It is obvious that this method leads to an image of poorer quality $f_l[u,v]$, where (u,v) depict the spatial coordinates on the low resolution grid. A high visual quality, however, is always preferred. Therefore, as in [5] proposed, a low resolution sensor can be covered with a non-regular sampling mask which can be seen on the right. Each large pixel of the low resolution sensor is divided into four quadrants, where three of them are randomly covered. As a consequence, only $1/4$ of the large pixel is sensitive to light anymore. This leads to an incomplete high resolution image, since due to the masking, pixels on the high resolution grid are only partially available. A suitable reconstruction algorithm is then needed for the reconstruction of these missing pixels. Finally, this leads to the reconstructed high resolution image $\hat{f}[m,n]$. Recently,

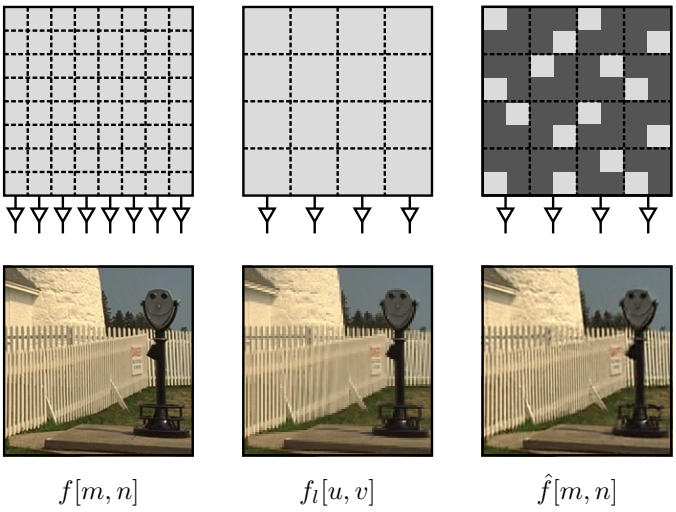


Figure 1. Left: High resolution sensor with many read-out circuits. Middle: Low resolution sensor with fewer read-out circuits and a poorer image quality. Right: Masked low resolution sensor giving a high resolution image after the reconstruction of all missing pixels.

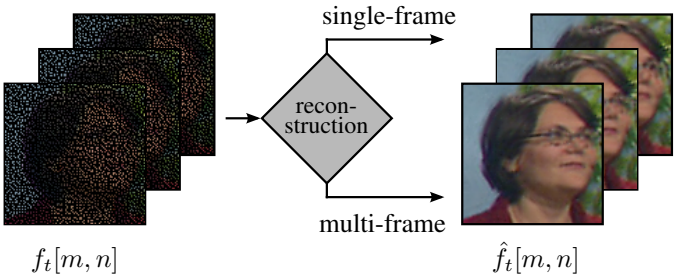


Figure 2. Non-regularly sampled video data $f_t[m,n]$ gets reconstructed either frame by frame (single-frame) or by utilizing motion information between the frames (multi-frame) in order to obtain the reconstructed high resolution video $\hat{f}_t[m,n]$.

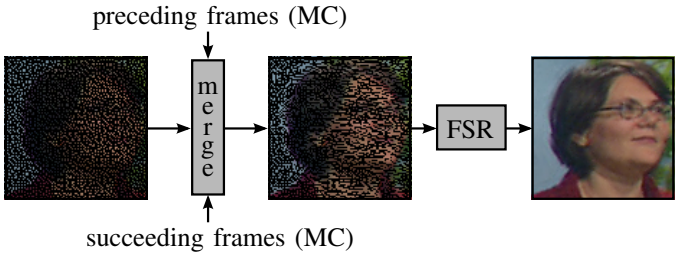


Figure 3. Merging of several frames after motion compensation (MC) to the current frame in order to obtain additional pixel information. Final reconstruction by frequency selective reconstruction (FSR).

it has been shown in [6] that the reconstruction quality of images captured by non-regular sampling sensors in multi-view scenarios may be further enhanced by utilizing the spatial correlation between neighboring views. When dealing with videos, the temporal correlation between neighboring frames may also be exploited as it is done for instance in an existing multi-frame reconstruction approach [7], in super-resolution [8], or video coding [9].

In this paper, a new recursive multi-frame reconstruction approach is proposed in order to increase the reconstruction quality compared to the existing multi-frame approach from [7]. This is achieved by introducing a new reference order. Up to now, the existing multi-frame approach employs a pre-reconstruction step, where all frames get reconstructed in the first place followed by a pixel-based motion estimation algorithm that is applied between all of these frames. The new reference order uses only preceding frames which allows the algorithm to be capable of real-time processing and additionally, due to a modified motion estimation, where motion vectors can be computed between a reconstructed frame and an incomplete non-regularly sampled frame, the pre-reconstruction step of the existing multi-frame approach can be avoided. Another advantage is the reusing of previously reconstructed frames for a subsequent motion estimation which leads to more reliable results of the computed motion vectors that are used for projecting pixels from one frame into another. Additionally, a new weighting function is introduced in order to incorporate the projected pixel information from different neighboring frames when they are projected onto the same position.

The paper is organized as follows: The next section introduces state-of-the-art methods for the reconstruction of non-regularly sampled videos and Section III presents the proposed recursive multi-frame reconstruction approach. Simulations and results are given in Section IV and Section V concludes this contribution.

II. State-of-the-art video reconstruction

In Figure 2, a scene is captured by a non-regular sampling sensor with a fixed sampling pattern giving a video which consists of incomplete frames $f_t[m,n]$. It contains many missing pixels due to the masking and has to be reconstructed in order to obtain the reconstructed high resolution frames $\hat{f}_t[m,n]$. A straightforward way is a single-frame reconstruction approach where each frame is reconstructed separately by a suitable reconstruction algorithm. A more sophisticated way is a multi-frame reconstruction, where motion information between neighboring frames is utilized in order to support the reconstruction of each frame.

A. Single-frame reconstruction

A frame-wise reconstruction of the sampled video can be conducted by several algorithms like Natural Neighbor Interpolation [10], Steering Kernel Regression [11], the constrained split augmented Lagrangian shrinkage algorithm [12], or sparsity-based wavelet inpainting [13]. However, it has been shown in [14] that for non-regular subsampling problems like this, frequency selective reconstruction (FSR) yields a better reconstruction quality than the other state-of-the-art image reconstruction algorithms. Recently, a texture-dependent approach for FSR has been developed [15], however, in this contribution only FSR from [14] is regarded. The reconstruction of single frames by FSR is called FSR-SF. The basic principle of FSR is the iterative generation of the sparse signal model

$$g_t[m,n] = \sum_{(k,l)\in\mathcal{K}} \hat{c}_{(k,l)} \varphi_{(k,l)}[m,n] \tag{1}$$

as a superposition of Fourier basis functions $\varphi_{(k,l)}[m,n]$ weighted by the expansion coefficients $\hat{c}_{(k,l)}$. This is done in a block-wise manner for each frame of the video. The set $\mathcal{K}$ contains the indices of all basis functions that have been selected for model generation. In every iteration, one basis function gets chosen and before being added to the model, its corresponding weight is estimated. The model $g_t[m,n]$ is then used to replace missing pixels in the corresponding high resolution frame $f_t[m,n]$.

B. Multi-frame reconstruction

For the reconstruction of a non-regularly sampled video, however, it is obviously advantageous to make use of the temporal dependencies between neighboring frames. Since the performance of FSR highly depends on the number of available sampling points, a multi-frame FSR approach (FSR-MF) has been proposed in [7] in order to increase the reconstruction quality. It projects additional pixel information from neighboring frames by using a suitable motion estimation algorithm.

First, all frames get reconstructed by the single-frame reconstruction approach FSR-SF. Afterwards, a modified block-based motion estimation [16] is applied between them, where the relative displacement is represented by a motion vector which is computed for each pixel. These motion vectors are then used to project pixel information from one frame into a neighboring frame. In Figure 3, this process is exemplarily shown. After a certain number of preceding and succeeding frames are motion compensated to the current frame, all valid pixel information is merged into a new frame which now contains less missing pixels. Finally, FSR is applied to obtain the reconstructed high resolution frame. These steps have to be repeated for all frames in order to get the reconstructed high resolution video.

III. Proposed Recursive Multi-Frame Reconstruction Approach

In this paper, a new recursive multi-frame reconstruction approach (FSR-RMF) is proposed in order to further increase the reconstruction quality compared to the existing multi-frame approach FSR-MF. It consists of two major parts: a new reference order for the motion estimation and a weighting function to incorporate multiple projected pixels.

A. Reference Order for Motion Estimation

First, the new reference order for motion estimation is introduced. The general principle is illustrated in Figure 4. Instead of utilizing both preceding and succeeding frames, only preceding frames are considered. In doing so, a real-time processing of the reconstruction of non-regularly sampled videos can be achieved. Additionally, motion estimation is now carried out between the non-regularly sampled current frame $f_t[m,n]$ and a certain number of previously reconstructed frames $\hat{f}_{t-k}[m,n]$. This way, a pre-reconstruction as it is done in the existing FSR-MF can be avoided. The motion estimation works the same way as in [7], however, missing pixels are now neglected for the matching. Another advantage of this new approach is that motion estimation can be applied between the non-regularly sampled current frame and preceding frames that are of higher quality, since they already have been reconstructed using pixel information from other preceding frames. Therefore, motion estimation and the projection of pixels using the corresponding motion vectors perform better, since more reliable pixel information is available.

The first frame $f_{t-3}[m,n]$ in this example has no preceding frames and is therefore directly reconstructed by FSR and saved as the reconstructed high resolution frame $\hat{f}_{t-3}[m,n]$. Now, the succeeding incomplete frame $f_{t-2}[m,n]$ has to be reconstructed. In this case, one preceding frame $\hat{f}_{t-3}[m,n]$ is available. Motion estimation can be carried out between them and pixel information can be projected. The final reconstruction by FSR leads to the reconstructed frame $\hat{f}_{t-2}[m,n]$. Analogously, this is done for all other frames of the non-regularly sampled video data, where a maximum number K of support frames is utilized.

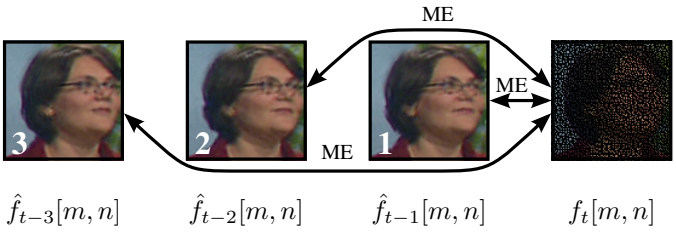


Figure 4. New reference order of the motion estimation (ME) between the non-regularly sampled current frame $f_t[m,n]$ and a certain number of previously reconstructed preceding frames $\hat{f}_{t-k}[m,n]$.

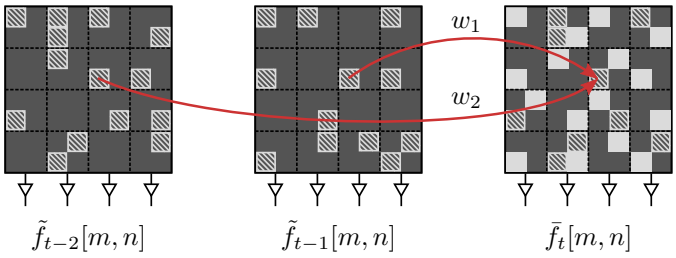


Figure 5. Merging and weighting of projected pixels from preceding motion compensated frames $\tilde{f}_{t-k}[m,n]$ into the current frame to be reconstructed.

B. Weighting of Projected Pixels from Neighboring Frames

The existing FSR-MF approach projects pixels from neighboring frames into the frame that is currently reconstructed. Up to now, if pixels from different frames are projected onto the same position, only the information from the nearest frame is used. It is now proposed to gather all pixels and weight them depending on the temporal distance to the current frame. The merged current frame $\bar{f}_t[m,n]$ is computed using the following formula

$$\bar{f}_t[m,n] = f_t[m,n] + \frac{\sum_{k=1}^{K} w_k \cdot \tilde{f}_{t-k}[m,n] \cdot b[m,n]}{\sum_{k=1}^{K} w_k} \tag{2}$$

with

$$b[m,n] = \begin{cases} 0 & \forall\ (m,n) \in \mathcal{A} \\ 1 & \forall\ (m,n) \in \mathcal{B} \end{cases}. \tag{3}$$

Depending on the number of utilized support frames K, all of the frames $f_{t-k}[m,n]$ are motion compensated to the current frame $f_t[m,n]$ and denoted by $\tilde{f}_{t-k}[m,n]$. $b[m,n]$ ensures that only pixels are projected which are not originally acquired by the non-regular sampling sensor, where $\mathcal{B}$ denotes the area of all missing pixels and $\mathcal{A}$ the area of all available pixels. All projected and merged pixels get weighted by the factor w_k depending on the temporal distance to the current frame.

An example for the merging and weighting of the projection of two support frames is shown in Figure 5. All originally acquired pixels are denoted by light-gray blocks and all motion compensated pixels by shaded blocks. All motion compensated frames $\tilde{f}_{t-k}[m,n]$ are merged with the current frame $f_t[m,n]$, however, only on positions with missing pixel information. This merged frame $\bar{f}_t[m,n]$ now has additional pixels which will support the reconstruction by FSR.

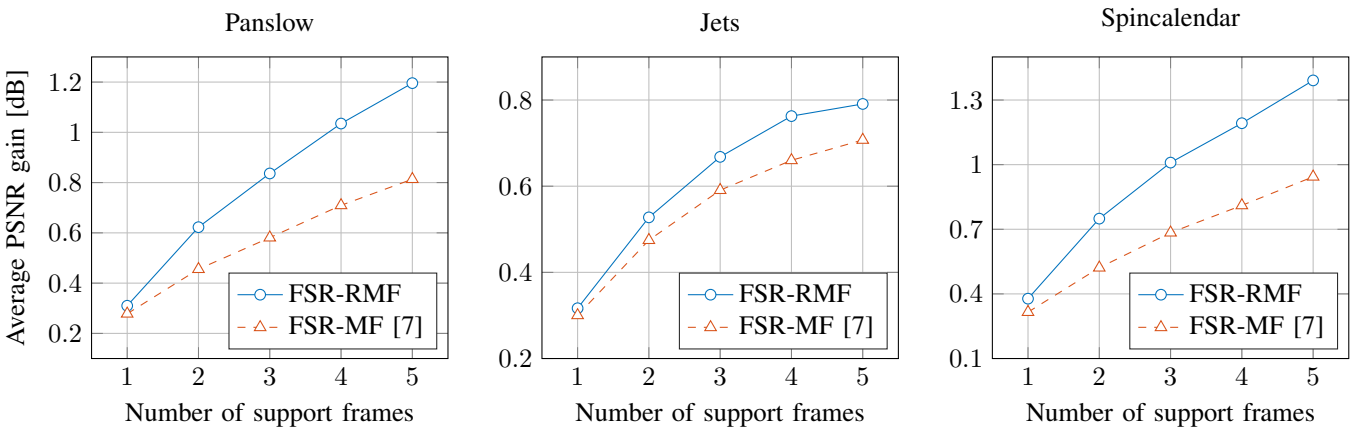


Figure 6. Average PSNR gain for FSR-MF and FSR-RMF each compared to FSR-SF over the number of support frames for three different test sequences.

Table I
FSR PARAMETERS USED DURING SIMULATION.

Block size	4×4
Border width	14
FFT size	32×32
Iterations	100
Decay factor $\hat{\rho}$	0.7
Orthogonality deficiency compensation γ	0.5
Weighting of already reconstructed areas δ	0.5

IV. SIMULATIONS & RESULTS

The proposed FSR-RMF is evaluated for three 720p test sequences, where only the luminance is considered. Each sequence has a different kind of motion: translation (*Panslow*), zoom (*Jets*), and rotation (*Spincalendar*). By selecting the first 100 frames of each sequence, a comprehensive test set of 300 frames is used. A fixed non-regular sampling mask is applied to every frame of each sequence and all frames are then reconstructed using the single-frame approach FSR-SF [14], the multi-frame approach FSR-MF [7] and the proposed FSR-RMF. All relevant parameters for FSR that are used during simulation are listed in Table I. For an extensive discussion of these parameters please refer to [14]. Since first tests have been shown that an equal weighting of projected pixels gives better results than a linearly decreasing weighting, FSR-RMF employs an equal weighting for all simulations.

The reconstruction quality of the different methods is evaluated using both PSNR and SSIM [17]. The corresponding values are calculated between the original frame and the reconstructed frame. Afterwards, the gain of FSR-RMF and FSR-MF is calculated with respect to FSR-SF. Furthermore, a margin of 4 pixels is excluded in order to avoid the influence of artifacts due to the black border of some frames. For both FSR-RMF and FSR-MF, up to five support frames are used.

In Figure 6, the average gain in PSNR for both FSR-RMF and FSR-MF is plotted over the number of utilized support frames. It can be seen that for each sequence the proposed FSR-RMF gives better results than the existing FSR-MF. It is also noticeable that the more support frames are utilized, the higher the overall gains get. Table II shows the average PSNR gains over all frames of all sequences for up to five utilized support frames. It can be seen that FSR-RMF leads to a better reconstruction quality for any number of support frames. For three support frames, the proposed FSR-RMF already performs slightly better than FSR-MF with five support frames. Compared to the single-frame reconstruction FSR-SF, FSR-RMF achieves an average gain in PSNR of up to 1.13 dB which is 0.31 dB better than to FSR-MF. In Table III, average SSIM gains are displayed. They show the same behavior as the PSNR results and verify the high reconstruction quality of the proposed FSR-RMF.

Table II
PSNR GAINS OF FSR-MF AND THE PROPOSED FSR-RMF EACH COMPARED TO FSR-SF AVERAGED OVER ALL FRAMES OF ALL SEQUENCES FOR UP TO FIVE SUPPORT FRAMES.

Support frames	1	2	3	4	5	
FSR-MF [7]	0.30	0.48	0.62	0.73	0.82	dB
FSR-RMF	0.34	0.63	0.84	1.00	**1.13**	dB

Table III
SSIM GAINS OF FSR-MF AND THE PROPOSED FSR-RMF EACH COMPARED TO FSR-SF AVERAGED OVER ALL FRAMES OF ALL SEQUENCES FOR UP TO FIVE SUPPORT FRAMES.

Support frames	1	2	3	4	5	
FSR-MF [7]	0.94	1.60	2.33	2.91	3.42	$\times 10^{-3}$
FSR-RMF	1.08	2.24	3.19	3.98	**4.63**	$\times 10^{-3}$

Three detail examples are shown in Figure 7, allowing a visual comparison of the proposed FSR-RMF with the existing FSR-MF. For both methods five support frames are utilized and the corresponding PSNR values are calculated on the entire frame. In the upper row, the original frames of the detail examples can be seen. The middle row shows how FSR-MF is able to reconstruct the non-regularly sampled frames and the last row shows the results for the proposed FSR-RMF. In the *Panslow* frame, it can clearly be seen that using FSR-RMF, more high frequency parts can be reconstructed. In the *Jets* frame, the text appear sharper and in the *Spincalendar* frame, fine details are better reconstructed and text is also better readable. Therefore, it can be stated that not only noticeable gains in PSNR and SSIM can be achieved, but also the visual quality gets significantly increased.

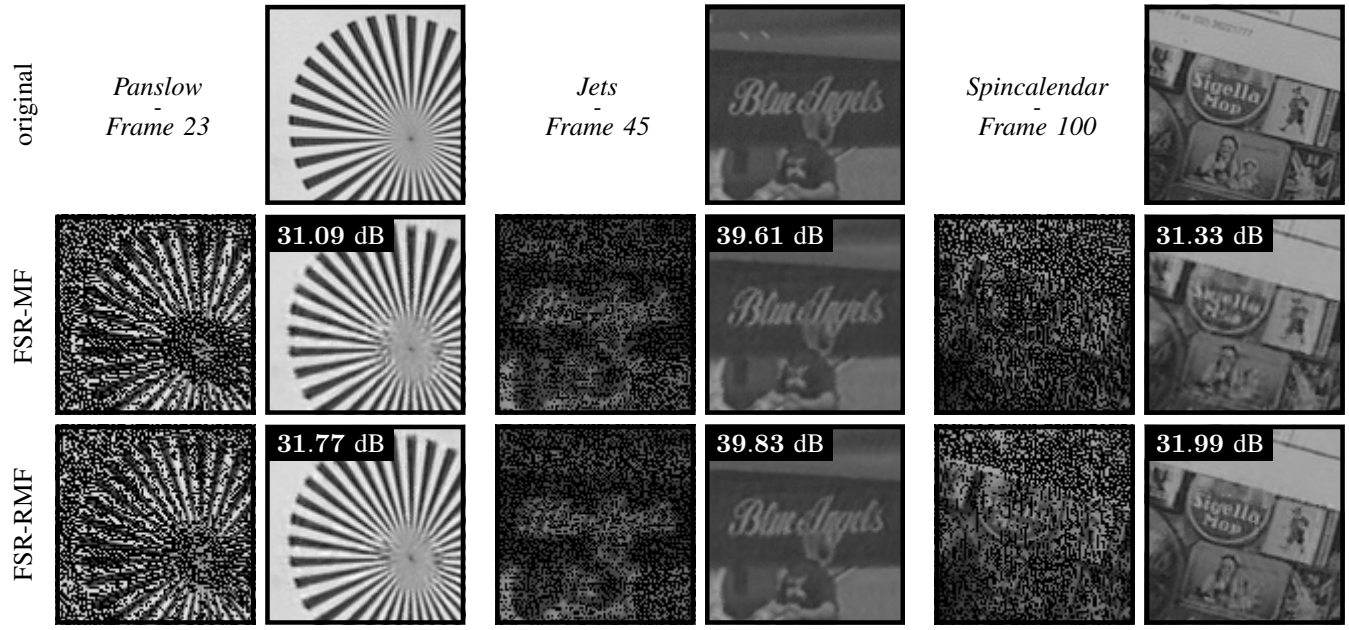


Figure 7. Detail examples of different frames for a visual comparison of the performance of both FSR-MF and the proposed FSR-RMF using five support frames. PSNR values are measured on the entire frame.

V. Conclusion

In this paper, the new recursive multi-frame reconstruction approach FSR-RMF has been proposed. FSR-RMF is able to reconstruct a video that is captured by a non-regular sampling sensor by utilizing pixel information from neighboring frames. It uses a new reference order which allows the reusing of previously reconstructed frames for motion estimation which leads to better results for the pixel projection. Compared to the existing multi-frame approach FSR-MF, a pre-reconstruction step can be avoided and a real-time processing is in general possible. Additionally, a new weighting function has been introduced in order to incorporate multiple pixels that are projected onto the same position. By employing the new FSR-RMF, a visually noticeable average gain in PSNR of up to 0.31 dB compared to the existing FSR-MF has been achieved. For future research, the influence of alternating non-regular sampling patterns over time will be investigated and a detailed evaluation of different weighting functions is also of great interest.

Acknowledgment

This work has been supported by the Deutsche Forschungsgemeinschaft (DFG) under contract number KA 926/5-3.

References

[1] M. Unser, "Sampling - 50 Years after Shannon," *Proc. of the IEEE*, vol. 88, no. 4, pp. 569–587, Apr. 2000.

[2] E. J. Candès and M. B. Wakin, "An Introduction To Compressive Sampling," *IEEE Signal Processing Magazine*, vol. 25, no. 2, pp. 21–30, Mar. 2008.

[3] D. L. Donoho, "Compressed Sensing," *IEEE Trans. on Information Theory*, vol. 52, no. 4, pp. 1289–1306, Apr. 2006.

[4] M. F. Duarte, M. A. Davenport, D. Takbar, J. N. Laska, T. Sun, K. F. Kelly, and R. G. Baraniuk, "Single-Pixel Imaging via Compressive Sampling," *IEEE Signal Processing Magazine*, vol. 25, no. 2, pp. 83–91, Mar. 2008.

[5] M. Schöberl, J. Seiler, S. Fößel, and A. Kaup, "Increasing Imaging Resolution by Covering Your Sensor," in *Proc. IEEE Int. Conf. on Image Processing (ICIP)*, Brussels, Belgium, Sep. 2011, pp. 1937–1940.

[6] M. Jonscher, J. Seiler, T. Richter, M. Bätz, and A. Kaup, "Reconstruction of Images Taken by a Pair of Non-Regular Sampling Sensors Using Correlation Based Matching," in *Proc. IEEE Int. Conf. on Image Processing (ICIP)*, Paris, France, Oct. 2014, pp. 2879–2882.

[7] M. Jonscher, J. Seiler, M. Bätz, T. Richter, W. Schnurrer, and A. Kaup, "Reconstruction of Videos Taken by a Non-Regular Sampling Sensor," in *Proc. IEEE Visual Communications and Image Processing (VCIP)*, Singapore, Singapore, Dec. 2015, pp. 1–4.

[8] S. C. Park, M. K. Park, and M. G. Kang, "Super-Resolution Image Reconstruction: A Technical Overview," *IEEE Signal Processing Magazine*, vol. 20, no. 3, pp. 21–36, May 2003.

[9] G. J. Sullivan, J.-R. Ohm, W.-J. Han, and T. Wiegand, "Overview of the High Efficiency Video Coding (HEVC) Standard," *IEEE Trans. on Circuits and Systems for Video Technology*, vol. 22, pp. 1649–1668, Sep. 2012.

[10] R. Sibson, "A Brief Description of Natural Neighbor Interpolation," in *Interpreting Multivariate Data*. John Wiley & Sons, 1981, pp. 21–36.

[11] H. Takeda, S. Farsiu, and P. Milanfar, "Kernel Regression for Image Processing and Reconstruction," *IEEE Trans. on Image Processing*, vol. 16, no. 2, pp. 349–366, Feb. 2007.

[12] M. V. Afonso, J. M. Bioucas-Dias, and M. A. T. Figueiredo, "An Augmented Lagrangian Approach to the Constrained Optimization Formulation of Imaging Inverse Problems," *IEEE Trans. on Image Processing*, vol. 20, no. 3, pp. 681–695, Mar. 2011.

[13] J.-L. Starck, F. Murtagh, and J. Fadili, *Sparse Image and Signal Processing: Wavelets, Curvelets, Morphological Diversity*. New York, NY, USA: Cambridge University Press, 2010.

[14] J. Seiler, M. Jonscher, M. Schöberl, and A. Kaup, "Resampling Images to a Regular Grid from a Non-Regular Subset of Pixel Positions Using Frequency Selective Reconstruction," *IEEE Trans. on Image Processing*, vol. 24, no. 11, pp. 4540–4555, Nov. 2015.

[15] M. Jonscher, J. Seiler, and A. Kaup, "Texture-Dependent Frequency Selective Reconstruction of Non-Regularly Sampled Images," in *submitted to Proc. Picture Coding Symposium (PCS)*, Nuremberg, Germany, Dec. 2016.

[16] M. Santamaría and M. Trujillo, "A Comparison of Block-Matching Motion Estimation Algorithms," in *Proc. IEEE 7th Colombian Computing Congress*, Medellín, Colombia, Oct. 2012, pp. 1–6.

[17] Z. Wang, A. Bovik, H. Sheikh, and E. Simoncelli, "Image Quality Assessment: From Error Visibility to Structural Similarity," *IEEE Trans. on Image Processing*, vol. 13, no. 4, pp. 600–612, Apr. 2004.